Sensors and Actuators B 136 (2009) 230–234

Contents lists available at ScienceDirect

Sensors and Actuators B: Chemical

journal homepage: www.elsevier.com/locate/snb

Two mechanisms of conduction in polycrystalline SnO_2 ☆

C. Malagù [a,*], M.C. Carotta [a], A. Giberti [a], V. Guidi [a], G. Martinelli [a], M.A. Ponce [b], M.S. Castro [b], C.M. Aldao [b]

[a] Department of Physics University of Ferrara, Via Saragat 1/C, I-44100 Ferrara, Italy
[b] Institute of Materials Science and Technology (INTEMA), Universidad Nacional de Mar del Plata-CONICET, Juan B. Justo 4302, B7608FDQ Mar del Plata, Argentina

ARTICLE INFO

Article history:
Received 28 July 2008
Received in revised form
29 September 2008
Accepted 21 October 2008
Available online 30 October 2008

Keywords:
Metal-oxide semiconductors
Tunneling
Impedance spectroscopy

ABSTRACT

Impedance spectroscopy was carried out on SnO_2 thick films exposed to different atmospheres. Oxygen desorption and adsorption during heating and cooling processes, respectively, onto the grain surface affects the resistance and electrical capacitance of the sensors. Double parabolic Schottky-type potential barriers at grain boundaries were assumed to analyze the tunneling and thermionic contributions to conductivity. In addition, the influence of the temperature on the oxygen diffusion into the grains annihilating oxygen vacancies was studied. It was deduced that in-diffusion substantially affects the conductivity.

© 2008 Elsevier B.V. All rights reserved.

1. Introduction

In the last two decades, gas sensors based on SnO_2 thick films became the dominant solid state devices for the gas detection in domestic, commercial, and industrial alarms [1,2]. It is generally accepted that, when oxygen chemisorbs, electrons transfer from the bulk to the surface of the grain modifying the barriers at the grain boundaries [3]. In particular, after oxygen adsorption, the barrier height and the depletion width become larger and, as a consequence, the sample resistance increases. Different factors (such as type of defects, morphology, and additives) contribute to the electrical response of the gas sensor [4–6].

The film conductivity is broadly used to characterize a sensor. Less attention has been paid to the electrical capacitance. Nevertheless, adsorption of gaseous species on the grain boundaries induces changes in the sensor apparent capacitance [7]. Indeed, for non-overlapped Schottky barriers (when the grain diameter is greater than the depletion layer $R \gg \Lambda$), the capacitance (C_{gb}) is related to the electron concentration in the bulk, N_d, and the potential barrier height, V_s, as [7]

$$C_{gb} \propto (N_d/V_s)^{1/2}. \quad (1)$$

Therefore, a decrease of the capacitance can be related to a higher barrier and/or to the reduction of the donor concentration due to the annihilation of oxygen vacancies.

In this work, the resistance and electrical capacitance response of an undoped tin oxide thick film gas sensor is analyzed as a function of temperature in an oxygen atmosphere. In order to explain these results, an electrical equivalent circuit that includes four different contributions to the overall impedance: grain boundary, bulk, electrode contact and the deep bulk traps presence was considered (see Fig. 2). Thermionic and tunneling contributions to electrical conduction have been considered to estimate the V_s and N_d.

2. Experimental

Analytical grades of $SnCl_2{\cdot}2H_2O$ (Baker) were employed as a tin source. Tin dioxide was precipitated at pH 6.25 through dropwise addition of ammonium hydroxide (NH_4OH) to an acid (HNO_3) solution of tin (II) chloride. A series of washings with deionised water were carried out until negative reaction of the filtrate with a concentrated silver nitrate ($AgNO_3$) solution. The obtained slurry, along with the required amounts of the dissolved additives, was added to a solution of citric acid in ethylene glycol in a 1:4 molar ratio. The mixtures were left at room temperature with constant stirring during 24 h aging with the purpose of promoting the formation of the metallic citrates. Later, a concentrated solution of NH_4OH was slowly added until a crystalline solution was attained which was afterwards evaporated and heated to promote the polymerization. The solid was heated to 350 °C for 12 h in the beaker to burn off the

☆ Paper presented at the International Meeting of Chemical Sensors 2008 (IMCS-12), July 13–16, 2008, Columbus, OH, USA.

* Corresponding author.
E-mail address: malagu@fe.infn.it (C. Malagù).

0925-4005/$ – see front matter © 2008 Elsevier B.V. All rights reserved.
doi:10.1016/j.snb.2008.10.015

organics compounds. The resulting black brittle mass was ground, transferred into an alumina crucible of large surface and thermally treated in an oven at 650 °C for 4 h. An X-ray powder diffraction (XRD) analysis was carried out with a Philips (PW1830) equipment running with CoKα radiation.

Thick and porous film samples were made mixing the powders with glycerol in a 2:1 ratio and by painting, with the obtained paste onto insulating alumina substrate on which gold electrodes with an interdigit shape had been deposited by sputtering. Finally, samples were thermally treated during 2 h in air at 500 °C. The mean thickness of the films was ~100 μm, as measured using a coordinates measuring machine Mitutoyo BH506. A Jeol JSM-6460LV microscope under the secondary electrons mode (SE) was employed to image the tin oxide surfaces. An impedance analyzer HP4191A, in the frequency range of 10^{-2} Hz to 15 MHz, was used. The system was linked to a computer for programming the measurements (100, 250, 350, 400, 425 °C) and for storing and handling the data. Z' vs. $-Z''$ curves were measured at different temperatures in air atmosphere (159.6 mmHg of oxygen). Temperature was increased and then decreased the temperature from 100 °C up to 450 °C at a rate of ~1 °C/min. Later, the decreasing was done from 450 °C to 100 °C at the same rate.

Experimental data were fitted with an $R(RC)$ equivalent circuit using the software Zview 2.1 for Windows. From temperature cycling experiments, the impedance response was obtained.

3. Results and discussion

3.1. Sample microstructure

Particle size distributions of the powders were determined by the Serigraph technique with a Micromeritics equipment. Table 1 shows data from particle size distributions corresponding to the SnO_2 powder obtained from the $SnCl_2{\cdot}2H_2O$ (Baker). We have considered that D80, D50 and D20 are the corresponding diameters of 80, 50 and 20% volume respectively, and $W = (D80 - D20)/D50$ is a measure of the distribution width of particle size. Later, the powder mass was ground and films were made. The film microstructure was analyzed with the scanning electron microscopy (SEM) technique (Fig. 1a), and a highly porous microstructure with agglomerates of 250 nm was observed. From Fig. 1b, the average particle size (that conform an agglomerate structure) was determined to be between 10 and 50 nm. From the XRD analysis the only presence of crystalline SnO_2 was detected as it is shown in Fig. 2a. The average particle size was also determinate using the Scherrer formula,

$$t = \frac{0.9\lambda}{B\cos(\theta_B)} \quad (2)$$

where t, the SnO_2 particle size; λ, the wavelength of the used radiation (Co = 1.7899 Å); B is the angular width (as $2\theta_B$) and is usually measured in radians, at an intensity equal to half the maximum intensity (9.5429×10^{-3} rad); and θ_B the angular value of the most intensity diffraction line shown in Fig. 2b. The particle size obtained was ~18 nm and this value is in good concordance with the results observed by the use of SEM.

Table 1
Particle size distributions of the obtained powders of SnO_2.

Sample	D20 (μm)	D50 (μm)	D80 (μm)	W
SnO_2	0.7	3	10	3.1

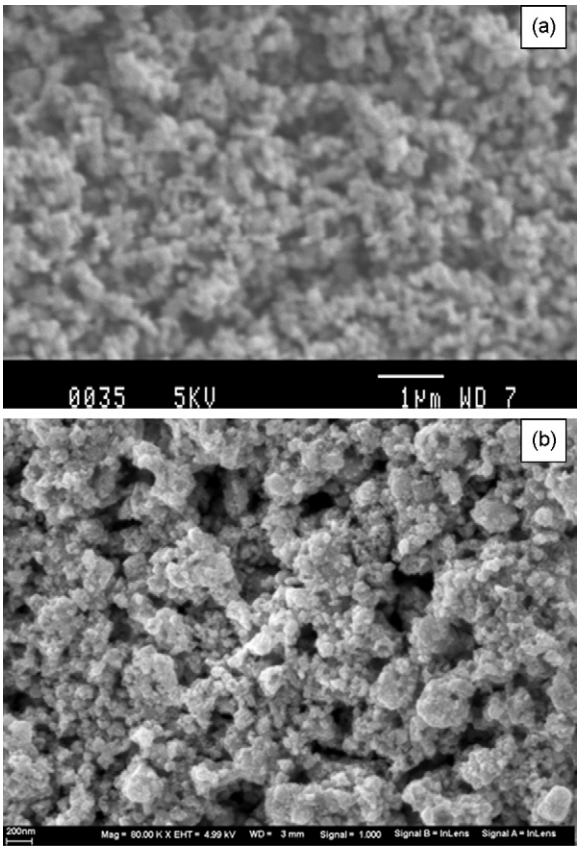

Fig. 1. Film microstructure was analyzed with the scanning electron microscopy (SEM) technique (a) bar = 1 μm (b) bar = 200 nm. A highly porous microstructure with agglomerates of 250 nm is observed.

3.2. Impedance interpretation and electronic equivalent circuit

It is well known that the interaction between oxygen and grain surfaces produces the transfer of electrons from the bulk to the surface [8]. From this process, barrier heights become larger and, as a consequence, the sample resistance increases.

When instead the sample temperature is modified at a fixed atmosphere the dominant effect is the change in the donors level as observed in [8]. In Fig. 1 the impedance was measured by raising and then decreasing the temperature under 159.6 mmHg of oxygen (dry air atmosphere). In this figure the evolution of the system is shown. It can be observed that the radius of the resulting semi-circles becomes smaller with increasing temperature. This indicates that grain-boundary resistance decreases with temperature, effect that is expected since current transport mechanisms are all thermally facilitated.

To analyze the impedance spectroscopy results, in Fig. 3 the considered electrical equivalent circuit is shown. R_{gb} and C_{gb} represent the grain-boundary resistance and capacitance, respectively. R_b and C_b represent the bulk resistance and capacitance, respectively. The electrode elements are R_e and C_e. R_t represents the deep bulk traps resistance [7]. Also, deviations in the Debye-like behavior were considered by using a constant phase element (CPE) in the equivalent circuit. To corroborate the above considerations, fittings were carried out with the proposed model of Fig. 4.

Very frequently, for a better analysis of the impedance measurements, the imaginary component of complex capacitance as $C''(\omega) = Z'/(\omega(Z'^2 + Z''^2))$ and the real component of the capacitance as $C'(\omega) = Z''/(\omega(Z'^2 + Z''^2))$ are calculated [8]. In a previous work we propose an alternative study in which the total parallel equivalent

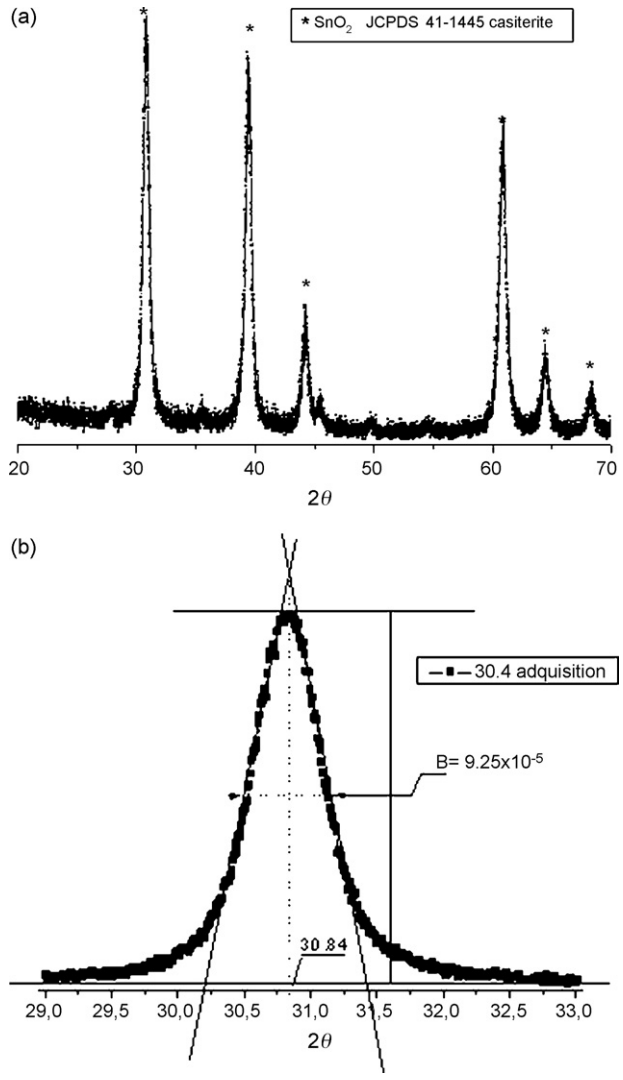

Fig. 2. X-ray powder diffraction. (a) High quality diffraction patterns, in the range 20–80° (2θ) the only presence of crystalline casiteritte is observed, (b) most intensity diffraction peak.

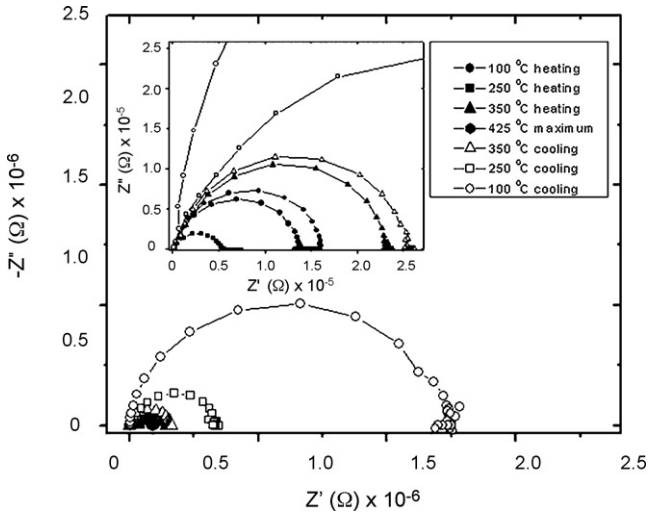

Fig. 3. Nyquist plot of the measured impedance of the sample measured by raising and then decreasing the temperature under oxygen atmosphere (159.6 mmHg).

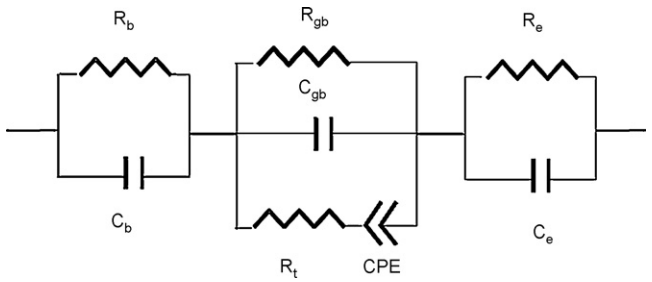

Fig. 4. Equivalent circuit employed to fit the data.

capacitance (C_p) and the total parallel resistance (R_p) as a function of frequency are analyzed [9–11].

In Fig. 5, the fittings of the C_p and R_p responses with frequency at 250 °C are shown. The capacitance fitting plot as a function of frequency at 250 °C in oxygen atmosphere considering the electrical equivalent circuit proposed in Fig. 4 is shown in Fig. 5a and the resistance fitting plot as a function of frequency at the same temperature is shown in

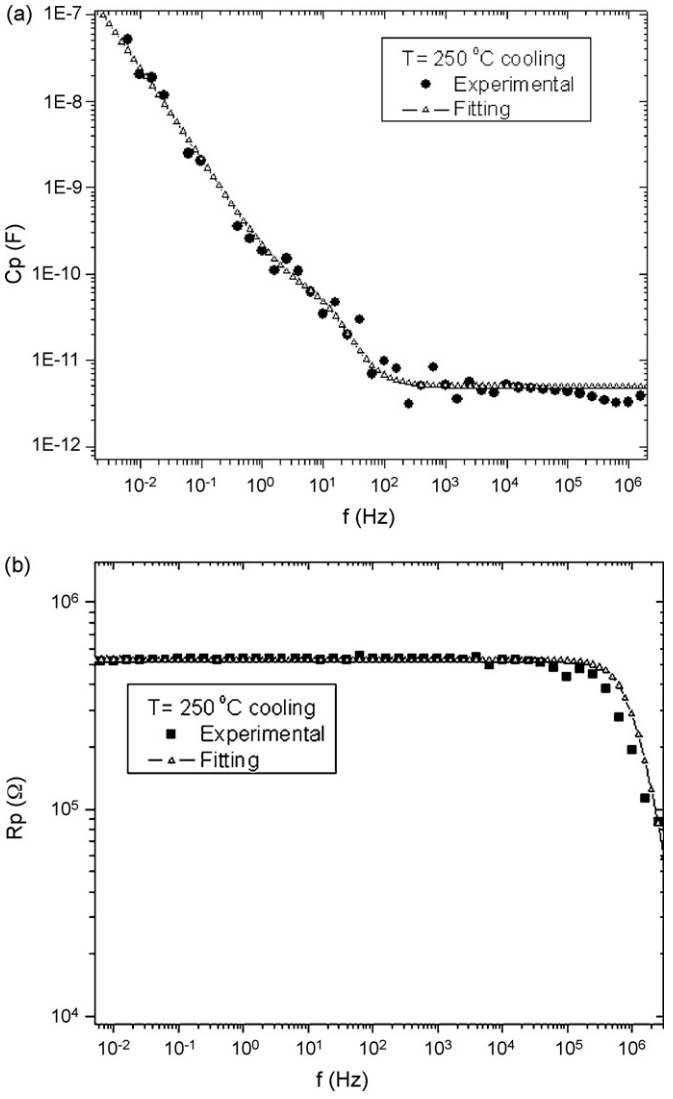

Fig. 5. (a) Capacitance fitting plots as a function of frequency at 250 °C in oxygen atmosphere. (b) Resistance fitting plots as a function of frequency at 250 °C in oxygen atmosphere.

Table 2
Grain boundaries resistance (R_{gb}) and capacitance (C_{gb}) as a function of temperature. V_s and N_d variations were calculated assuming thermionic and tunneling contributions to electrical conduction.

	100 °C	250 °C	350 °C
$R_{gb(initial)}$ (kΩ)	167.683	62.087	161.542
$R_{gb(final)}$ (kΩ)	1871.151	561.398	437.395
$C_{gb(initial)}$ (pF)	3.38	4.72	4.61
$C_{gb(final)}$ (pF)	2.69	3.84	4.39
$V_{s(initial)}$ (eV)	1.00	0.95	1.00
$V_{s(final)}$ (eV)	1.06	1.027	1.05
$N_{d(initial)}$ (m^{-3})	10^{24}	1.5×10^{24}	10^{24}
$N_{d(final)}$ (m^{-3})	6.7×10^{23}	8.12×10^{23}	9.56×10^{23}
$J_{total(initial)}$ (A/cm^2)	3.60×10^{-6}	6.61×10^{-2}	0.5186
$J_{total(final)}$ (A/cm^2)	3.31×10^{-7}	7.28×10^{-3}	0.1857

Fig. 5b. The employed elements values were $C_{gb} = 3.84 \times 10^{-12}$ F, $R_{gb} \approx 5.3 \times 10^5\ \Omega$, $CPE_{(1-a)} = 0.2$, $CPE_{(A)} = 5 \times 10^{-8}$, $R_t = 5 \times 10^7\ \Omega$, $C_e = 1 \times 10^{-5}$ F, $R_e = 1100\ \Omega$, $C_b = 5 \times 10^{-14}$ F and $R_b = 1600\ \Omega$. Also, using the proposed model of Fig. 2, fittings for 350 and 425 °C were carried out [9]. Now, to develop a method to calculate the values of N_d, we focalize in the R_{gb} and C_{gb} values of the circuit elements obtained from these fittings. The R_{gb} and C_{gb} values for the overall temperature cycle are shown in Table 2.

3.3. Calculation of the currents (two mechanisms)

By solving the Poisson's equation under the depletion approximation or resorting to the Gauss theorem, the grain-boundary barrier height (eV_s) and width (Λ) are directly related as follows [10].

$$eV_s = \frac{e^2 N_d}{2\varepsilon} \Lambda^2 \left(1 - \frac{2\Lambda}{3R}\right) \tag{3}$$

where R is radius of the particle, Λ the depletion layer width and N_d is the donor density. Schottky barrier heights are around 1 eV and the donor density is in the order of 10^{24} m^{-3} [10]. With these values, the critical grain size (diameter) for which the grains are completely depleted is ~110 nm. From SEM microscopy a microstructure of 250 nm agglomerate particles diameter was observed. Thus, initially, grains cannot present overlapped potential barriers. But, after the thermal treatment in an air atmosphere at 500 °C, some grains are expected to have a donor concentration lower than 10^{24} m^{-3} due to oxygen vacancies annihilation. In Fig. 5 the evolution of the grain-boundary resistance and capacitance during a temperature cycle are shown (A to B for resistance and C to D for capacitance). The final resistance, after the cycle is completed, is higher than the initial one. Conversely, the final capacitance becomes lower than the initial one. These changes in the grain-boundary resistance and capacitance can be associated with the modification of the barrier heights and of the donor concentration. In a Schottky barrier the capacitance is related to the donor concentration in the bulk, N_d, and the barrier height, V_s, as it was shown in Eq. (1).

The diminution of the final capacity then can be related to a higher barrier, to the reduction of the donor concentration due to the annihilation of oxygen vacancies after the oxygen diffusion into the grains, or to both phenomena simultaneously. Thus, the ratio between the initial and final grain-boundary capacitances can be expressed as follows [7]:

$$\left(\frac{C_i}{C_f}\right)^2 = \frac{N_{di}}{N_{df}} \frac{V_{sf}}{V_{si}}, \tag{4}$$

where N_{di} is the initial donor concentration in the bulk (during the heating), N_{df} is the final donor concentration in the bulk (during the cooling), V_{si} and V_{sf} correspond to the initial and final barriers heights, respectively. We found that the ratio between initial and final grain-boundary resistances and capacitances at $T = 100$ °C, for example, is $R_i/R_f = 0.0896$ and $C_i/C_f = 1.256$. Thus, using Eq. (3), the ratio between initial and final N_d and V_s can be expressed as follows.

$$\frac{N_{di}}{N_{df}} \frac{V_{sf}}{V_{si}} = 1.578 \tag{5}$$

After the oxygen treatment we expect a reduction in the donor concentration and a significant change in the sample resistance. The total current density over and through a barrier can be calculated as:

$$J = \frac{AT}{k} \int_0^{V_s} f(E) P(E)\, dE + AT^2 \exp\left(\frac{-V_s}{kT}\right) \tag{6}$$

where the first term corresponds to the tunneling current and the second to the thermionic current, A and k are the Richardson and Boltzmann constants, and $f(E)$ is the Fermi-Dirac distribution. $P(E)$, the transmission probability for a reverse-biased Schottky barrier (which is the limiting step), is given by

$$P(E) = \left\{ \exp - \left[\frac{4\pi V_s}{qh} \left(\frac{m\varepsilon}{N_d}\right)^{1/2} \ln\left(1 - \frac{(1-\beta)^{1/2}}{\beta^{1/2}}\right) \right] \right\}, \tag{7}$$

where m is the electron effective mass, ε the electrical permittivity, h the Planck constant and β is E/V_s [10].

Assuming reasonable starting values for V_s (1 eV) and N_d (10^{24} m^{-3}) we found that, for example at 100 °C, the barrier height must increase about 0.06 eV and simultaneously the donor concentration must decrease about 33%. These findings are consistent with oxygen adsorption and diffusion into the grains reported in a previous work [7,8]. Oxygen diffuses into the grains and annihilates oxygen vacancies, the donor concentration decrease resulting in an enlargement of the depletion layer. These effects produce an increasing of the grain-boundary resistance. In all the temperature range of our studies, the tunneling current is calculated to be more than an order of magnitude larger than the thermionic current.

When the temperature is increased, the final electrical resistance measured at low frequencies at 250 °C (561.398 ohms according to Table 2) is higher than its initial value at 100 °C (167.683 ohms according to Table 2). This increase in the intergrain resistance can be associated with a modification in the barrier heights or to a decrease of doping level (an increase of conductance was expected due to the increasing temperature). In the experimental conditions in which the sample is exposed to oxygen and the temperature changes, a variation in the barrier width is also possible. These results are consistent with those previously reported for polycrystalline semiconductors [12,13]. Fig. 6 shows that, contrarily to what was observed for the grain-boundary resistance value, the grain-boundary capacitance increases with the sole temperature. Considering Eq. (1), a change of the final capacity can be related to a variation of the donor concentration due to the annihilation or the creation of oxygen vacancies after an atmosphere change.

Finally, in Table 2, the evolution of the total current (corresponding to the addition of tunnel and thermionic currents) at three different temperatures during the cycle is presented. Furthermore, using Eqs. (3)–(7), we calculated the evolution of the potential barrier height and the donor concentration values. In Table 2, it is observed that the final barrier height is always higher than the initial one. Conversely, after the cycle, the donor concentration becomes smaller.

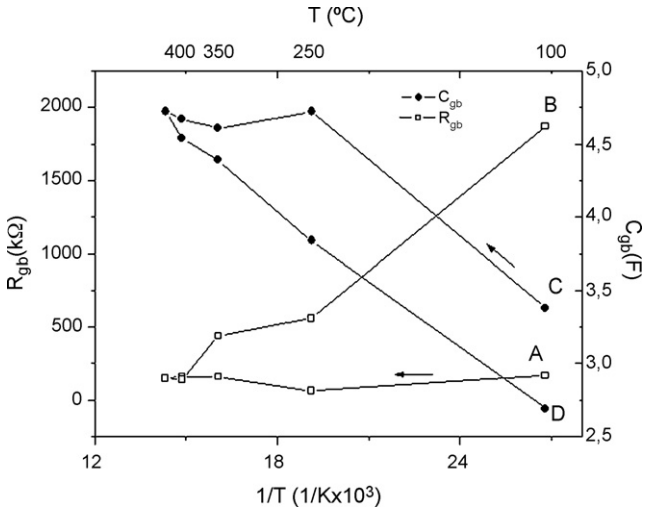

Fig. 6. R_{gb} and C_{gb} derived from the model as functions of operating temperature.

4. Conclusions

In this work we present a model for tunneling and thermionic barrier crossing in polycrystalline semiconductors. The model was employed to analyze the impedance spectroscopic response of SnO_2 to different gaseous atmospheres. The spherical approximation of the grains leads to Eq. (3) the solution of which, putting the experimental values as input, results in an interesting outcome: the effect of the lower doping level due to oxygen in-diffusion predominates. Indeed, the large increase in the resistance accompanied by the relatively low decrease in the capacitance results in a narrower depletion region which indicates a decrease in N_d. Thus, unexpectedly, it is necessary for the density of surface states, after oxygen exposure, to be lower in order to account for a quasi constant surface barrier and Λ can only increase.

Acknowledgements

The authors express their thanks to CONICET, CNR, the University of Ferrara and the University of Mar del Plata for the financial support, to Jorge Rodríguez Páez and Alejandra Montenegro (University of Cauca, Colombia) for the powders preparation and to Adrián Cristobal for the technical support with DRX measurements.

References

[1] W. Göpel, K.D. Schierbaum, SnO_2 sensors: current status and future prospects, Sens. Actuators B Chem. 26–27 (1995) 1–12.
[2] N. Barsan, U. Weimar, Conduction model of metal oxide gas sensors, J. Electroceram. 7 (2001) 143–167.
[3] G. Gaggiotti, A. Galkidas, S. Kaciulis, G. Mattogno, A. Setkus, Surface chemistry of tin oxide based gas sensors, J. Appl. Phys. 76 (1994) 4467–4471.
[4] S. Capone, P. Siciliano, F. Quaranta, R. Rella, N. Epifani, L. Vasanelli, Moisture influence and geometry effect of Au and Pt electrodes on CO sensing response of SnO_2 microsensors based on Sol-Gel thin film, Sens. Actuators B Chem. 3911 (2001) 1–9.
[5] C. Xu, J. Tawaki, N. Miura, N. Yamazoe, Grain size effects on gas sensitivity of porous SnO_2-based elements, Sens. Actuators B Chem. 3 (1991) 147–155.
[6] M. Labeau, U. Schmatz, G. Delabouglise, J. Roman, M. Vallet-Regi, A. Gaskow, Capacitance effects and gaseous adsorption on pure and doped polycrystalline tin oxide, Sens. Actuators B Chem. 26–27 (1995) 49–52.
[7] M.A. Ponce, M.S. Castro, C.M. Aldao, Influence of oxygen adsorption and diffusion on the overlapping of intergranular potential barriers in SnO_2 thick-films, Mater. Sci. Eng. B 111 (2004) 14–19.
[8] G. Belmont, G.F. Fabregat-Santiango, Effect of trap density on the dielectric response of varistor ceramics, Solid State Electronics 43 (1999) 2123.
[9] M.A. Ponce, M.S. Castro, C.M. Aldao, Capacitance and Resistance measurements of SnO_2 thick films, J. Mater Sci. Mat. Electron. DOI 10.1007/s 10854-008-9590-8.
[10] M.A. Ponce, C. Malagù, M.C. Carotta, G. Martinelli, C.M. Aldao, Gas in-diffusion contribution to impedance in tin oxide thick films, J. Appl. Phys. 104 (2008) 054907.
[11] C. Malagù, V. Guidi, M.C. Carotta, G. Martinelli, Unpinning of the Fermi level and tunneling in metal oxide semiconductors, Appl. Phys. Lett. 84 (21) (2004) 4158–4160.
[12] C.R. Crowell, V.L. Rideout, Normalized thermionic-field (T-F) emission in metal-semiconductor (Schottky) barriers, Solid State Electronics 12 (1969) 89.
[13] M. Seitz, F. Hampton, W. Richmond, Influence of chemisorbed oxygen on the ac electrical behavior of polycrystalline ZnO, in: M.F. Yan, A.H. Heuer (Eds.), Advanced in Ceramics, vol. 7: Additives and Interfaces in Electronic Ceramics, 84th Annual Meeting of the American Ceramic Society, Cincinnati, Ohio, USA, May 1982, The American Ceramic Society Inc., Columbus, Ohio, USA, 1983, pp. 60–70.

Biographies

Cesare Malagù bachelor in Physics at the University of Ferrara in 1997, he got his PhD in 2001 in experimental physics. Post doc with the National Institute of Physics of Matter in 2001. His current research activity regards analytical modelling of polycrystalline semiconductors and photovoltaic technology. He is a lecturer at the University of Ferrara and teaches general physics at the Department of Chemistry.

Maria Cristina Carotta is a Doctor in Physics at Ferrara University (Italy). Since 1981 she has been researcher at the Department of Physics of the same University; she is also researcher within the Italian National Institute of Matter (INFM). Since 1983 she has focused her research on semiconductor physics, mainly on electrical, optical and transport properties of silicon and of semiconducting oxides for gas sensors. She is currently involved in research projects concerning the development of nanostructured thick film gas sensors for environmental pollutants monitoring.

Alessio Giberti bachelor in Physics at the University of Ferrara in 2000, he got his PhD in 2004 in experimental physics. Post doc with the National Institute of Physics of Matter he received a one year research grant starting from 2004. Research activity, carried out at the Sensors and Semiconductors laboratory of the University of Ferrara, is mainly based on the modelling of transport phenomena in nanostructured semiconductors. He is author of several papers in peer-reviewed journals and contributions to the proceedings of international conferences.

Vincenzo Guidi bachelor in Physics at the University of Ferrara in 1990, fellow at "Budker Institute for Nuclear Physics" of Novosibirsk (Russia) in 1991, PhD in 1994. Researcher then associate professor in experimental physics (FIS/01) since 1994 at the Faculty of Engineering of the University of Ferrara. Council member and scientific evaluator for the National Institute for Nuclear Physics (INFN) from 1999 to 2005. Research activity, carried out at the Sensors and Semiconductors laboratory of the University of Ferrara, has consisted of both investigations of basic phenomena in semiconductors and to practical implementations.

Giuliano Martinelli received his doctorate degree in physics at the University of Ferrara (Italy). Based at the Physics Department of the University of Ferrara as associate professor since 1980 and then as full professor; since 2000 he is the Director of the Physics Department of the University of Ferrara. He has been Advisor of several industries, mainly in U.S.A. (SOLEC Int., Los Angeles) and in Germany (Siemens Solar, Munich). In Italy he contributed to the installation of a plant (Helios Technology S.p.a., Padova) for the manufacturing of solar cells, modules and systems. His research interests include silicon crystals growth, photovoltaic technology and thick-film gas sensors. He co-ordinated several European projects both in P.V. and gas-sensor fields. He is a Member of I.N.F.M. (National Institute for the Physics of Matter) and he is in charge of Research at C.N.R. (National Council of Research) since 1975. He holds two international patents in the field of crystal growth (tri-crystal ingots) and thin solar cells.

Miguel Adolfo Ponce obtained his B.Sc. in Chemistry in 1999 and PhD in Material Science in 2005 from Mar del Plata National University, Argentina. Since April 2007 assistant researcher of CONICET. His current research interest includes the development of electronic conduction mechanism of functional inorganic materials.

Miriam Castro obtained her Chemical Engineering degree in 1988, and PhD in Materials Science in 1993 from Mar del Plata National University. Her current research interests include the development and application of functional inorganic materials.

Celso Manuel Aldao completed his PhD at the Department of Chemical Engineering and Materials Science of the University of Minnesota in 1989. After a postdoctoral stage in this department, he moved to the University of Mar del Plata where he was appointed as Professor. Since 1992 he is a member of the research staff of the National Research Council (CONICET). Aldao's research activities focus on the physics and chemistry of surfaces and interfaces, with special emphasis on semiconductors. He also works on different aspects of crystal growth modelling and diffusion, and electronic ceramics.